

SUPPORT INFORMATION

**All-green  $\text{Cs}_4\text{CuSb}_2\text{Cl}_{12}$  perovskite films deposited in situ by AACVD and their doping with F<sup>-</sup> ions for photodetectors and memdiodes.**

J.U. Balderas-Aguilar,<sup>a</sup> C. Falcony,<sup>b</sup> I.A. Garduño-Wilches,<sup>c</sup> M. Aguilar-Frutis,<sup>d</sup> N. Hernández-Como,<sup>e</sup> I.E. Martínez-Merlín,<sup>f</sup> M. García-Hipólito,<sup>a</sup> J.C. Alonso.<sup>a</sup>

<sup>a</sup> Instituto de Investigaciones en Materiales, Universidad Nacional Autónoma de México, Ciudad Universitaria, A.P. 70-360, Coyoacán, 04510, Mexico City, Mexico

E-mail: [jubalderas@im.unam.mx](mailto:jubalderas@im.unam.mx)

<sup>b</sup> Centro de Investigación y de Estudios Avanzados del IPN (CINVESTAV) Departamento de Física Av. Instituto Politécnico Nacional 2508, San Pedro Zacatenco Gustavo A. Madero CDMX, 07360, Mexico.

<sup>c</sup> CONAHCyT- Instituto Politécnico Nacional, Centro de Investigación en Ciencia Aplicada y Tecnología Avanzada, Calzada Legaria 694, Col. Irrigación, Alcaldía Miguel Hidalgo, C.P. 11500, México D.F., México.

<sup>d</sup> Instituto Politécnico Nacional, Centro de Investigación en Ciencia Aplicada y Tecnología Avanzada, Calzada Legaria 694, Col. Irrigación, Alcaldía Miguel Hidalgo, C.P. 11500, México D.F., México.

<sup>e</sup> Centro de Nanociencias y Micro y Nanotecnologías, Instituto Politécnico Nacional, Av. Luis Enrique Erro S/N, Unidad Profesional Adolfo López Mateos, Zacatenco, Alcaldía Gustavo A. Madero, C.P. 07738, Ciudad de México

<sup>f</sup> Tecnológico Nacional de México Instituto Tecnológico de Tlalnepantla DEPI,. Av. Instituto Tecnológico S/N Col. La Comunidad, Tlalnepantla de Baz 54070, México

### **Diffuse reflectance measurement details and optical bandgap calculation**

Diffuse reflectance spectra of the CCSC and CCSCF films deposited on top of glass substrates were measured using an integrating sphere under synchronous scan, i.e., both, excitation and emission monochromators are set to the same wavelength. To eliminate any optical signals originating from the glass substrate, the sample was enclosed within a Teflon mask that featured an open window. This design allowed only the surface of the perovskite films to be exposed while concealing the glass substrate from the excitation light. For optical bandgap determination from reflectance spectra, the procedure reported elsewhere was employed as follows:<sup>1</sup>

The CCSC and CCSCF reflectance spectra acquired were transformed into pseudo-absorbance spectra using the Kubelka-Munk equation:

$$\alpha = (1 - R) / (2R),$$

where R represents the reflectance, and  $\alpha$  stands for the pseudo-absorbance. Subsequently, a modified Kubelka-Munk function was determined by multiplying  $\alpha$  by the photon energy  $hv$ , incorporating the relevant coefficient n associated with an electronic transition:

$$\alpha^*hv,$$

with n equaling 2 for direct transitions. To determine the band gaps, a linear portion of the plot ( $\alpha^* hv$ )<sup>2</sup> against E (photon energy) was fitted, and the x-intercept was used for extraction.

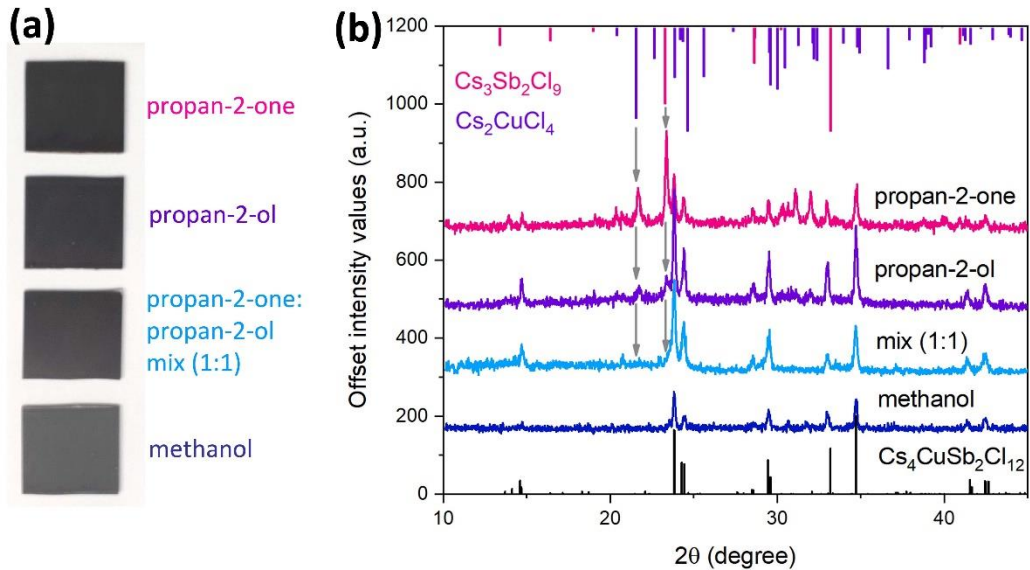


**Figure S1.** Digital photographs taken under ambient light illumination of four  $\text{Cs}_4\text{CuSb}_2\text{Cl}_{12}$  films deposited by AACVD using different solvent conditions for the  $\text{CuCl}_2 - \text{SbCl}_3$  precursor solution (a), and their respective X-ray diffractograms (b). The diffraction patterns for the  $\text{Cs}_4\text{CuSb}_2\text{Cl}_{12}$  (black lines),  $\text{Cs}_3\text{Sb}_2\text{Cl}_9$  (pink lines), and  $\text{Cs}_2\text{CuCl}_4$  (purple lines) were simulated from CIF data.

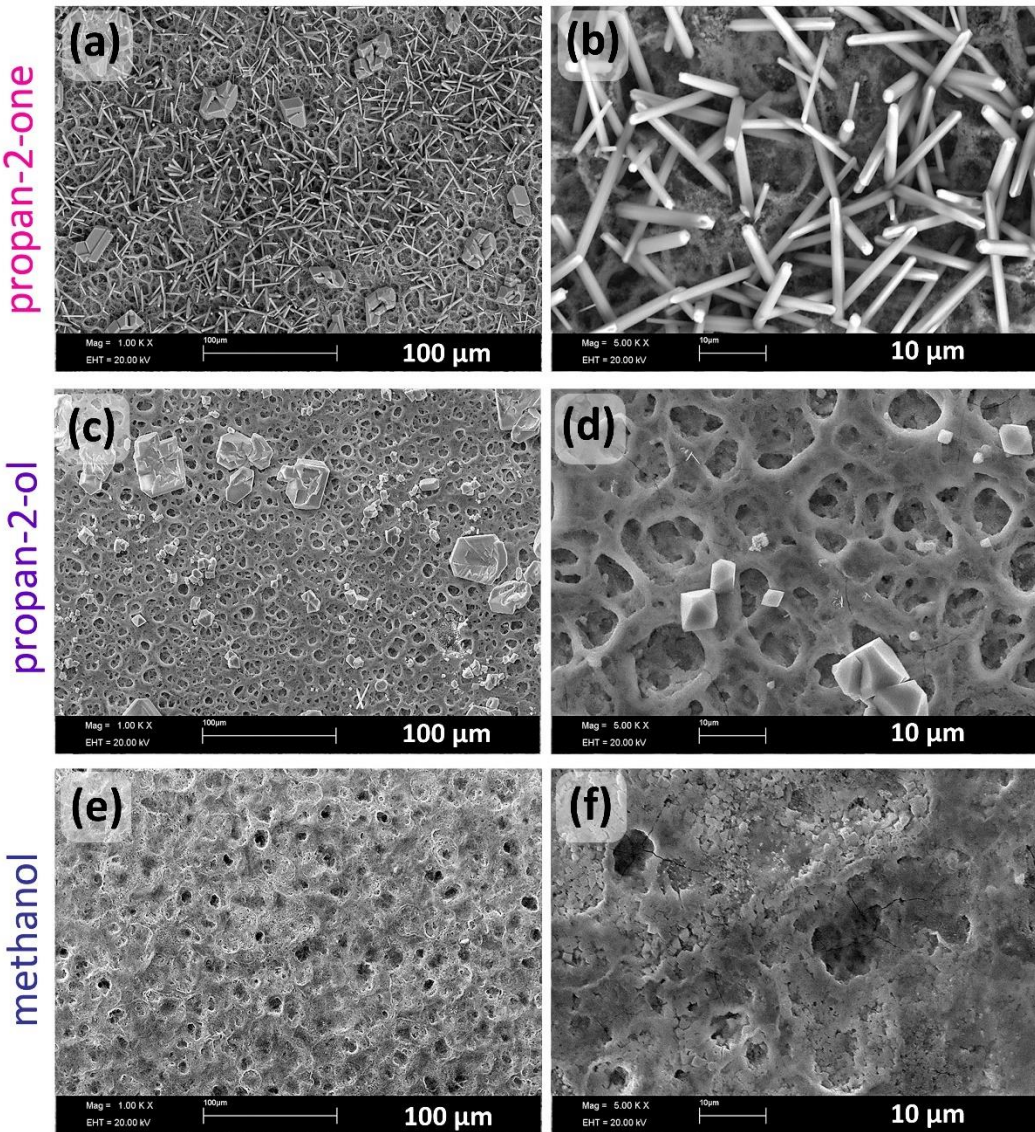


**Figure S2.** SEM images at different magnifications of the films using propan-2-one (a-b), propan-2-ol (c-d), and methanol (e-f), as solvents for the  $\text{CuCl}_2 - \text{SbCl}_3$  precursor solution.

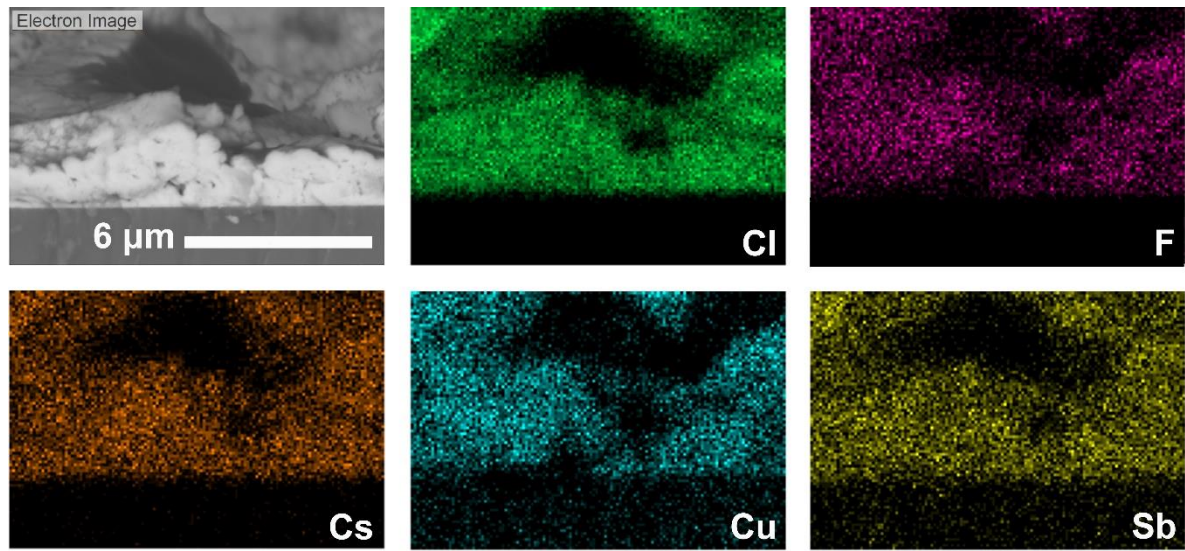


**Figure S3.** Cross-sectional SEM image of the CCSCF film mapped area and the elemental mapping of the Cl, F, Cs, Cu, and Sb elements.

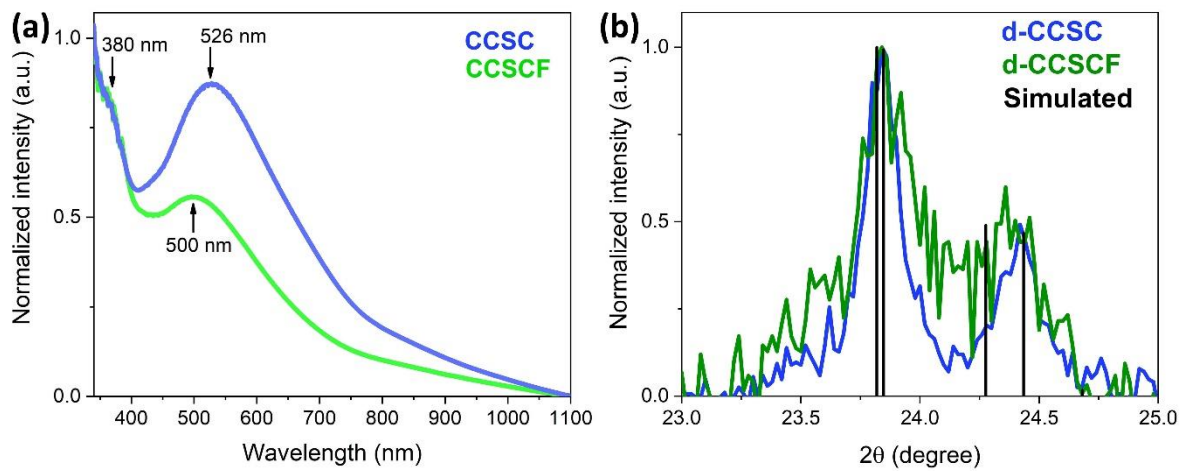


**Figure S4.** Normalized UV-Vis-NIR absorbance spectra of the CCSC and CCSCF films (a). Normalized diffraction patterns of the d-CCSC and d-CCSCF films, along with the simulated diffraction pattern from CIF data (b).

**Table S1.** Solubilities (g/100 g solvent) of the precursor salts in the respective solvents used in this study.

	<b>water</b>	<b>methanol</b>	<b>propan-2-one</b>	<b>propan-2-ol</b>
<b>CsCl</b>	186.5 (20 °C) <sup>2</sup>	3.39 (18 °C) <sup>3</sup>		
<b>CuCl<sub>2</sub></b>			2.97 (18 °C) <sup>4</sup>	19 (40 °C) <sup>5</sup>
<b>SbCl<sub>3</sub></b>			537.6 (18 °C) <sup>6</sup>	Soluble <sup>7</sup>
<b>SbF<sub>3</sub></b>			70 (25°C) <sup>5</sup>	42.7 (25°C) <sup>5</sup>

**Table S2.** Undoped  $\text{Cs}_4\text{CuSb}_2\text{Cl}_{12}$  bandgap values reported for different crystal presentations.

Presentation	Eg (eV)	Ref
Microcrystals	1.02	<sup>1</sup>
Microcrystals	1.14	<sup>8</sup>
Nanocrystals	1.6	<sup>9</sup>
Nanocrystals	1.79	<sup>10</sup>
Microcrystals	1.16	<sup>11</sup>
Nanocrystals	1.56	<sup>12</sup>
Nanocrystals	1.92	<sup>13</sup>
Nanocrystals	1.96	<sup>14</sup>
Nanocrystals	1.67	<sup>15</sup>
Microcrystals	1.4	<sup>15</sup>
Microcrystals	1.32	<sup>16</sup>
Nanocrystals	2.2	<sup>16</sup>
Single crystal	1.13	<sup>17</sup>
Microcrystals	1.66	<sup>18</sup>
Film	1.65	This work

**Table S3.** Electrical characteristics of metal halide perovskite materials

Sample	Mobility (cm <sup>2</sup> /Vs)	Carrier density (cm <sup>-3</sup> )	Conductivity (S/cm)	Method	Ref.
Cs <sub>4</sub> CuSb <sub>2</sub> Cl <sub>12</sub> nanocrystals	2.5 (electrons) 2.5 (holes)	-	.	Input parameter in device modelling and simulation	19, 20
FA <sub>0.83</sub> Cs <sub>0.17</sub> Pb(I <sub>0.9</sub> Br <sub>0.1</sub> ) <sub>3</sub> polycrystalline films	0.04 – 1.4 (sum of electrons and holes)	-	-	Time resolved microwave conductivity (TRMC)	21
(FA <sub>0.83</sub> MA <sub>0.17</sub> ) <sub>0.95</sub> Cs <sub>0.05</sub> Pb(I <sub>0.9</sub> Br <sub>0.1</sub> ) <sub>3</sub>	0.3 – 6.7 (electrons and holes)	1.1x10 <sup>14</sup>	1 x 10 <sup>-5</sup>	TRMC	21
(C <sub>6</sub> H <sub>5</sub> C <sub>2</sub> H <sub>4</sub> NH <sub>3</sub> ) <sub>2</sub> SnI <sub>4</sub> film (2D)	0.6 (holes)	-	-	Field effect transistor (FET)	2223
PEASnI <sub>4</sub> film (2D)	15 (holes)	-	-	(FET)	2324
MAn <sub>-1</sub> PEA <sub>2</sub> Pb <sub>n</sub> I <sub>3n+1</sub> film (2D)	6-11 (electrons and holes)			Optical pump probe spectroscopy	23
MAPbI <sub>3</sub> thin films	8 – 35 (electrons and holes)		-	Space Charge Limited current (SCLC), Transient absorption spectroscopy, Hall Effect, FET	252627
$\alpha$ -phase FAPbI <sub>3</sub> thin film	1.1	1.3x10 <sup>16</sup>	1.1x10 <sup>-7</sup>		28
$\delta$ -phase FAPbI <sub>3</sub> single crystals	0.179	3.1x10 <sup>11</sup>	8.9x10 <sup>-9</sup>		28
MAPbI <sub>3-x</sub> Cl <sub>x</sub>	11.6	10 <sup>15</sup> -10 <sup>17</sup>	-		26
MAPbBr <sub>3</sub>	13	1x10 <sup>13</sup>		SCLC	29
MAPbI <sub>3</sub>	8	9x10 <sup>14</sup>	-	Hall and solid state photoconductivity	30
MAPbBr <sub>3</sub>	60	1x10 <sup>12</sup>	-	Hall and solid state photoconductivity	30
MAPbBr <sub>3</sub>	8	2x10 <sup>12</sup>		Hall	31
Cs <sub>4</sub> CuSb <sub>2</sub> Cl <sub>12</sub> :F film	0.4	1.65x10 <sup>15</sup>	1.94 x 10 <sup>-5</sup>	Hall	[This work]

ferences

- 1 B. Vargas, E. Ramos, E. Pérez-Gutiérrez, J. C. Alonso and D. Solis-Ibarra, A Direct Bandgap Copper-Antimony Halide Perovskite, *J Am Chem Soc*, 2017, **139**, 9116–9119.
- 2 V. A. Rabinovich and Z. Ya. Khavin, *Kratkii khimicheskii spravochnik (Concise Chemical Handbook)*, KHIMIIA Leningrad , 1991.
- 3 V. E. Plyushchev and B. D. Stepin, *Analiticheskaya khimiya rubidiua i tsesiya (Analytical Chemistry of Rubidium and Cesium)*, Moscow: Nauka, 1975.
- 4 Janz G.J and Tomkins R.P.T., *Nonaqueous Electrolytes Handbook*, Academic Press, New York and London, 1973, vol. 2.
- 5 V. B. Kogan, V. M. Fridman and V. V. Kafarov, *Spravochnik po rastvorimosti (Solubility Handbook)*, Nauk SSSR, 1961, vol. 1.
- 6 Seidell A., *Solubilities of inorganic and metal organic compounds.*, D. Van Nostrand Company, New York, 3rd edn., 1940, vol. 1.
- 7 N. León-Brito, A. Melendez, I. Ramos, N. J. Pinto and J. J. Santiago-Aviles, Electrical properties of electrospun Sb-doped tin oxide nanofibers, *J Phys Conf Ser*, 2007, **61**, 683–687.
- 8 N. Singhal, R. Chakraborty, P. Ghosh and A. Nag, Low-Bandgap Cs<sub>4</sub>CuSb<sub>2</sub>Cl<sub>12</sub> Layered Double Perovskite: Synthesis, Reversible Thermal Changes, and Magnetic Interaction, *Chem Asian J*, 2018, **13**, 2085–2092.
- 9 X. D. Wang, N. H. Miao, J. F. Liao, W. Q. Li, Y. Xie, J. Chen, Z. M. Sun, H. Y. Chen and D. Bin Kuang, The top-down synthesis of single-layered Cs<sub>4</sub>CuSb<sub>2</sub>Cl<sub>12</sub> halide perovskite nanocrystals for photoelectrochemical application, *Nanoscale*, 2019, **11**, 5180–5187.
- 10 T. Cai, W. Shi, S. Hwang, K. Kobbekaduwa, Y. Nagaoka, H. Yang, K. Hills-Kimball, H. Zhu, J. Wang, Z. Wang, Y. Liu, D. Su, J. Gao and O. Chen, Lead-Free Cs<sub>4</sub>CuSb<sub>2</sub>Cl<sub>12</sub> Layered Double Perovskite Nanocrystals, *J Am Chem Soc*, 2020, **142**, 11927–11936.
- 11 P. M. Jayasankar, A. K. Pathak, S. P. Madhusudanan, S. Murali and S. K. Batabyal, Double perovskite Cs<sub>4</sub>CuSb<sub>2</sub>Cl<sub>12</sub> microcrystalline device for cost effective photodetector applications, *Mater Lett*, , DOI:10.1016/j.matlet.2019.127200.
- 12 A. P. P. M. Joshi, D. Verma, S. Jadhav, A. R. Choudhury and D. Jana, Layered Cs<sub>4</sub>CuSb<sub>2</sub>Cl<sub>12</sub> Nanocrystals for Sunlight-Driven Photocatalytic Degradation of Pollutants, *ACS Appl Nano Mater*, 2021, **4**, 1305–1313.
- 13 T. Cai, W. Shi, D. J. Gosztola, K. Kobbekaduwa, H. Yang, N. Jin, Y. Nagaoka, L. Dube, J. Schneider, S. Hwang, J. Gao, X. Ma and O. Chen, Colloidal synthesis and charge carrier dynamics of Cs<sub>4</sub>Cd<sub>1-x</sub>Cu<sub>x</sub>Sb<sub>2</sub>Cl<sub>12</sub> ( $0 \leq x \leq 1$ ) layered double perovskite nanocrystals, *Matter*, 2021, **4**, 2936–2952.

- 14 A. Mandal, A. Mondal, R. Bhattacharyya and S. Bhattacharyya, Cs<sub>4</sub>CuSb<sub>2</sub>Cl<sub>12-x</sub>I<sub>x</sub> (x = 0–10) nanocrystals for visible light photodetection, *Nanotechnology*, , DOI:10.1088/1361-6528/ac7ed2.
- 15 D. Wu, C. Tian, J. Zhou, Y. Huang, J. Lai, B. Gao, P. He, Q. Huang and X. Tang, Morphology and structure of lead-free CuSb-based double perovskites for photocatalytic CO<sub>2</sub> reduction , *Carbon Neutralization*, 2022, **1**, 298–305.
- 16 S. Parveen, L. T. Manamel, A. Mukherjee, S. Sagar and B. C. Das, Analog Memristor of Lead-Free Cs<sub>4</sub>CuSb<sub>2</sub>Cl<sub>12</sub> Layered Double Perovskite Nanocrystals as Solid-State Electronic Synapse for Neuromorphic Computing, *Adv Mater Interfaces*, , DOI:10.1002/admi.202200562.
- 17 W. Zhou, P. Han, C. Luo, C. Li, J. Hou, Y. Yu and R. Lu, Band-Gap and Dimensional Engineering in Lead-Free Inorganic Halide Double Perovskite Cs<sub>4</sub>Cu<sub>1-x</sub>Ag<sub>2x</sub>Sb<sub>2</sub>Cl<sub>12</sub> Single Crystals and Nanocrystals, *Front Mater*, , DOI:10.3389/fmats.2022.855950.
- 18 S. Mishra, S. Sapru, S. N. Upadhyay, A. Singh, S. Pakhira and A. K. De, Elucidating the Structure-Property Relationship and Ultrafast Exciton/Charge Carrier Dynamics of Layered Cs<sub>4</sub>CuSb<sub>2</sub>Cl<sub>12</sub> Double-Perovskite Microcrystals, *Journal of Physical Chemistry C*, 2023, **127**, 1881–1890.
- 19 S. C. Yadav, V. Manjunath, A. Srivastava, R. S. Devan and P. M. Shirage, Stable lead-free Cs<sub>4</sub>CuSb<sub>2</sub>Cl<sub>12</sub> layered double perovskite solar cells yielding theoretical efficiency close to 30%, *Opt Mater (Amst)*, , DOI:10.1016/j.optmat.2022.112676.
- 20 Y. He, L. Xu, C. Yang, X. Guo and S. Li, Design and numerical investigation of a lead-free inorganic layered double perovskite cs<sub>4</sub>cusb<sub>2</sub>cl<sub>12</sub> nanocrystal solar cell by scaps-1d, *Nanomaterials*, , DOI:10.3390/nano11092321.
- 21 J. Lim, M. Kober-Czerny, Y. H. Lin, J. M. Ball, N. Sakai, E. A. Duijnstee, M. J. Hong, J. G. Labram, B. Wenger and H. J. Snaith, Long-range charge carrier mobility in metal halide perovskite thin-films and single crystals via transient photo-conductivity, *Nat Commun*, , DOI:10.1038/s41467-022-31569-w.
- 22 C. R. Kagan, D. B. Mitzi and C. D. Dimitrakopoulos, Organic-inorganic hybrid materials as semiconducting channels in thin- film field-effect transistors, *Science (1979)*, 1999, **286**, 945–947.
- 23 L. M. Herz, *ACS Energy Lett*, 2017, **2**, 1539–1548.
- 24 T. Matsushima, S. Hwang, A. S. D. Sandanayaka, C. Qin, S. Terakawa, T. Fujihara, M. Yahiro and C. Adachi, Solution-Processed Organic–Inorganic Perovskite Field-Effect Transistors with High Hole Mobilities, *Advanced Materials*, 2016, **28**, 10275–10281.
- 25 R. L. Milot, G. E. Eperon, H. J. Snaith, M. B. Johnston and L. M. Herz, Temperature-Dependent Charge-Carrier Dynamics in CH<sub>3</sub>NH<sub>3</sub>PbI<sub>3</sub> Perovskite Thin Films, *Adv Funct Mater*, 2015, **25**, 6218–6227.

- 26 C. Wehrenfennig, G. E. Eperon, M. B. Johnston, H. J. Snaith and L. M. Herz, High charge carrier mobilities and lifetimes in organolead trihalide perovskites, *Advanced Materials*, 2014, **26**, 1584–1589.
- 27 J. Peng, Y. Chen, K. Zheng, T. Pullerits and Z. Liang, *Chem Soc Rev*, 2017, **46**, 5714–5729.
- 28 Q. Han, S. H. Bae, P. Sun, Y. T. Hsieh, Y. Yang, Y. S. Rim, H. Zhao, Q. Chen, W. Shi, G. Li and Y. Yeng, Single Crystal Formamidinium Lead Iodide (FAPbI<sub>3</sub>): Insight into the Structural, Optical, and Electrical Properties, *Advanced Materials*, 2016, **28**, 2253–2258.
- 29 V. M. Le Corre, E. A. Duijnsteene, O. El Tambouli, J. M. Ball, H. J. Snaith, J. Lim and L. J. A. Koster, Revealing Charge Carrier Mobility and Defect Densities in Metal Halide Perovskites via Space-Charge-Limited Current Measurements, *ACS Energy Lett*, 2021, **6**, 1087–1094.
- 30 Y. Chen, H. T. Yi, X. Wu, R. Haroldson, Y. N. Gartstein, Y. I. Rodionov, K. S. Tikhonov, A. Zakhidov, X. Y. Zhu and V. Podzorov, Extended carrier lifetimes and diffusion in hybrid perovskites revealed by Hall effect and photoconductivity measurements, *Nat Commun*, , DOI:10.1038/ncomms12253.
- 31 H. T. Yi, X. Wu, X. Zhu and V. Podzorov, Intrinsic Charge Transport across Phase Transitions in Hybrid Organo-Inorganic Perovskites, *Advanced Materials*, 2016, **28**, 6509–6514.